Construction of a Flexibility Analysis Model for Flexible High-Throughput Satellite Communication Systems With a Digital Channelizer

Kazuma Kaneko, *Student Member, IEEE*, Hiroki Nishiyama, *Senior Member, IEEE*, Nei Kato, *Fellow, IEEE*, Amane Miura, *Member, IEEE*, and Morio Toyoshima, *Member, IEEE*

***Abstract*—Recent years have seen the development of a satellite communication system called a high-throughput satellite (HTS), which enables large-capacity communication to cope with various communication demands. Current HTSs have a fixed allocation of communication resources and cannot flexibly change this allocation during operation. Thus, effectively allocating communication resources for communication demands with a bias is not possible. Therefore, technology is being developed to add flexibility to satellite communication systems, but there is no system analysis model available to quantitatively evaluate the flexibility performance. In this study, we constructed a system analysis model to quantitatively evaluate the flexibility of a satellite communication system and used it to analyze a satellite communication system equipped with a digital channelizer.**

***Index Terms*—Digital channelizer, frequency flexibility, high-throughput satellite communication.**

I. Introduction

SATELLITE communication systems are expected to meet the rising demand for broadband communication from increased globalization because of their vast coverage area and ability to provide communication on the sea and in air. As the world enters the age of the Internet of Things (IoT), an enormous number of devices will be connected to each other, and satellite communication systems are expected to serve as a means of communication to such devices [1]–[4]. The unmanned aircraft system (UAS) has also attracted much attention, and various applications such as infrastructure inspection and environmental investigation are being studied [5]–[7]. However, a UA does not necessarily fly within the radio wave coverage of a terrestrial network. Not only do the data acquired by the aircraft need to be collected, but also controlling an unmanned aerial vehicle is difficult. Therefore, satellite communication systems are being considered as a means of communication with a UAS. In addition, satellite communication systems have been attracting attention as communication infrastructure for developing countries, and much research is being done on networks using multiple satellites [8], [9]. There are also examples of research that focused on light waves rather than radio waves to increase the capacity of satellite communication [10]. These systems can also be used as a communication method in emergency situations because of their disaster-resistant nature; even when large-scale disasters occur on Earth, satellite systems in outer space remain intact. Currently, demand is increasing for large-capacity communication such as high-quality video transmission in order to understand a disaster situation and implement an advanced disaster response, and satellite communication systems are required to meet these demands. In response to such communication demands, a satellite communication system called the High-Throughput Satellite (HTS) has been developed to further enable large-capacity communication [11]–[14]. For HTSs currently in practical use, the allocation of communication resources is fixed, and they cannot efficiently allocate resources to communication demands generated by various uses. Thus, the next generation of HTSs need frequency flexibility so that they can flexibly assign communication resources according to biases in communication [15]–[18]. Technology for adding flexibility to a satellite is being developed. One representative example is a digital channelizer [19]–[22]. However, there are no examples of research that has clearly defined flexibility for satellite communication and quantitatively evaluated it. In this study, we defined the flexibility required for a satellite communication system and constructed a system analysis model to evaluate it. In addition, we used the model to evaluate the flexibility of a satellite communication system with a digital channelizer.

The remainder of this paper is organized as follows. The supposed network model is explained in Section II. Section III presents the satellite communication system with the digital channelizer that was evaluated with the system analysis model. The channel assignment method is also explained in this section. Then, Section IV presents the mathematical analysis for the evaluation. Finally, the paper is concluded in Section V.

Manuscript received February 13, 2017; revised June 16, 2017; accepted July 23, 2017. Date of publication August 9, 2017; date of current version March 15, 2018. This work was supported in part by the Ministry of Internal Affairs and Communications, Japan, which was conducted under the national project, Research and Development of Bandwidth-on-Demand High Throughput Satellite Communications System. The review of this paper was coordinated by Dr. P. Lin. *(Corresponding author: Kazuma Kaneko.)*

K. Kaneko, H. Nishiyama, and N. Kato are with the Graduate School of Information Sciences, Tohoku University, Sendai 980-8576, Japan (e-mail: kazuma.kaneko@it.is.tohoku.ac.jp; hiroki.nishiyama.1983@ieee.org; kato@it.is.tohoku.ac.jp).

A. Miura and M. Toyoshima are with Wireless Network Research Institute, National Institute of Information and Communications Technology, Tokyo 184-8795, Japan (e-mail: amane@nict.go.jp; morio@nict.go.jp).

Digital Object Identifier 10.1109/TVT.2017.2736010

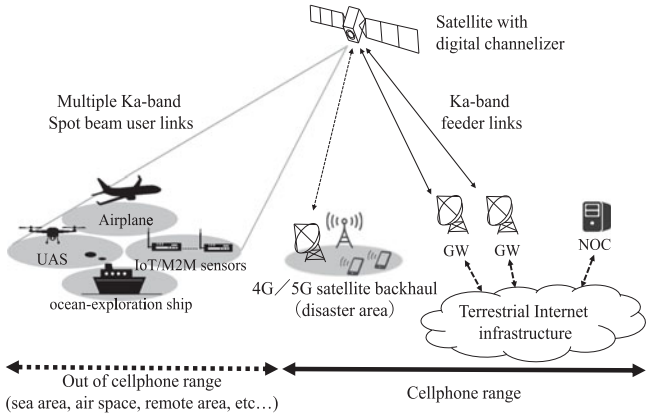

Fig. 1. Supposed satellite communication system.

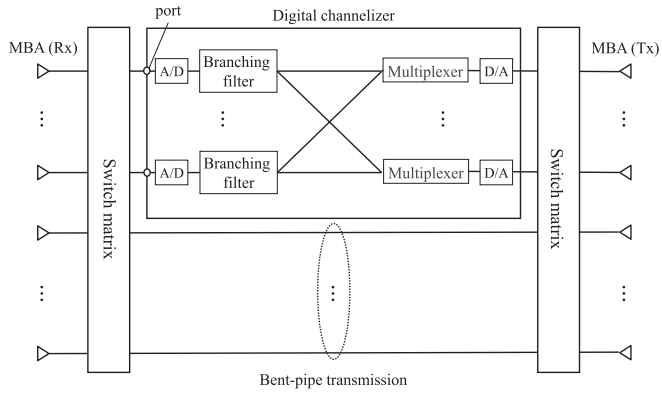

Fig. 2. Block diagram of the hybrid transponder.

II. Supposed Environment

In this section, we summarize the supposed environment. Then, we describe the functions of digital channelizer in detail.

A. System Configuration

Fig. 1 shows the supposed satellite communication system. The HTS has multiple Ka-band spot beams for user links and Ka-band feeder links.

We assumed that there are several gateways (GWs) in this network that are connected to a terrestrial network. The network operation center (NOC) manages the satellite communication resources. That is, channels are assigned according to communication requests from user terminals. To prevent interference, the satellite allocates different frequency bandwidths to adjacent spot beams. However, in order to improve the efficiency of frequency utilization, the satellite reuses the same frequency bandwidth to spot beams that are separated by a distance. When two spot beams are separated by a distance, the interference between two beams can be neglected [23]–[28].

B. Communication Types

We noticed a relationship between the satellite communication type and our system analysis model. There are two types of satellite communication: star and mesh [29], [30]. In star-type communication, all traffic is sent to a GW, even if the communication is between spot beams. Traffic, which generates a specific spot beam, and the destination, which is another spot beam, are sent to the GW through the satellite. Then, the traffic is sent to the destination spot beam from the GW through the satellite. Because the transponder has a simple structure that is suitable for satellite communication, a general satellite system is constructed based on star-type communication. On the other hand, traffic is sent to the other spot beam without going to the GW in mesh-type communication. The satellite directly downlinks traffic from the specific spot beam to the destination beam. In mesh-type communication, because the communication between beams does not use any feeder links, feeder links can be effectively utilized. Although conventional satellites do not adopt mesh-type communication because of mountability concerns, a digital channelizer makes it possible to simplify the transponder, so a satellite with digital channelizer can adopt mesh-type communication. Therefore, we constructed a system analysis model based on mesh-type communication. Next, we explain the assumed transponder of the satellite communication system. It is hard to process all frequency bandwidths with a digital channelizer on a satellite because of cost and mountability; the processing frequency bandwidth of an HTS sometimes reaches several tens of gigahertz. Therefore, we focused on a hybrid transponder that shares a bent-pipe mode and digital channelizer. Fig. 2 presents a block diagram of the hybrid transponder. Part of the input from the Multi-Beam Antenna (MBA) is processed by the digital channelizer and output, and the remaining inputs are processed by bent-pipe transmission. Because the assumed transponder uses mesh-type communication, the output is also made to the MBA. In this research, the signal input from the antenna was input from the channelizer port to the channelizer, and the channelizer port and input from the antenna had one-to-one correspondence. Therefore, the ratio of the signal processed by the channelizer and proportion of the bent-pipe transmission were determined by the number of ports of the channelizer. When the number of input antennas and number of ports of the channelizer are equal, this means that all of the signals are processed by the channelizer. We evaluated the influence of the number of ports of the digital channelizer on the flexibility of the system.

C. Function of Digital Channelizer

Here, we summarize the three functions of the digital channelizer and explain the function focused on in this study.

Because bent-pipe satellites cannot change the frequency bandwidth assigned to the spot beam, all spot beams are assigned a fixed frequency bandwidth. On the other hand, a digital channelizer can change the frequency bandwidth allocation between spot beams. In disaster situations, a satellite communication system with a digital channelizer can allocate a large frequency bandwidth to the spot beam covering the disaster area.

When the traffic destination is a specific GW, because a bent-pipe satellite simply downlinks the traffic from the user link channel to the feeder link channel, the number of feeder link channels is the sum of the user link channels, as illustrated in

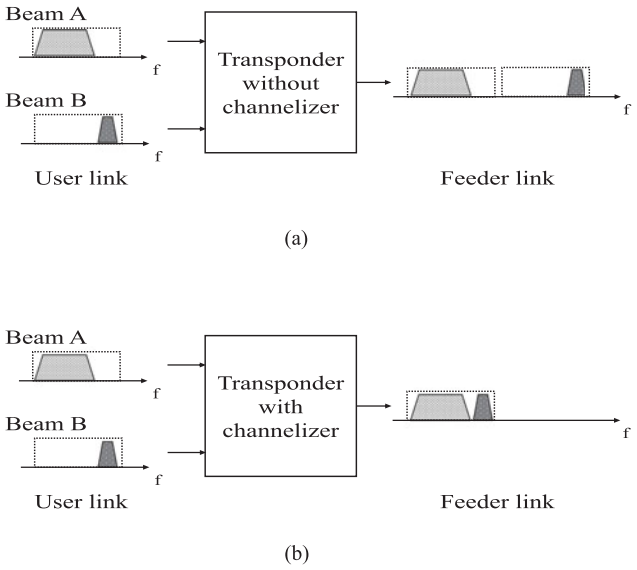

Fig. 3. Function of a digital channelizer for star-type communication. (a) Bent-pipe system. (b) Digital channelizer.

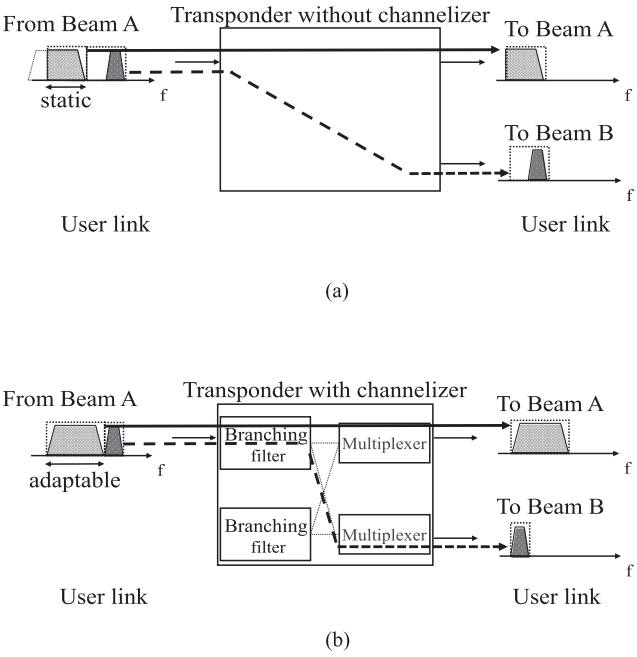

Fig. 4. Function of a digital channelizer for mesh-type communication. (a) Bent-pipe system. (b) Digital channelizer.

Fig. 3(a). When user terminals do not generate much traffic and there are many free channels on the user link, the feeder link becomes a wideband signal with many empty channels, as shown in Fig. 3(a). A satellite equipped with a digital channelizer can pick up data from the user link channel at the transponder and then multiplex the data on the feeder link channel to avoid generating idle channels, as shown in Fig. 3(b). Thus, a satellite equipped with a digital channelizer can improve the frequency utilization efficiency of the feeder link.

Fig. 4 presents an example of mesh-type communication. The satellite receives user link channels from beam A and sends these channels to beams A and B. When a large amount of traffic is generated from beam A to beam B, accommodating all of it is impossible even if there are other open channels, as shown in Fig. 4(a), because current bent-pipe satellites define a fixed frequency bandwidth for each destination beam. On the other hand, a digital channelizer can change the frequency bandwidth allocation for each destination beam. Thus, the NOC can optimize the channel allocation depending on the amount of generated traffic, as shown in Fig. 4(b). This study focused on this function to evaluate the improvement in flexibility.

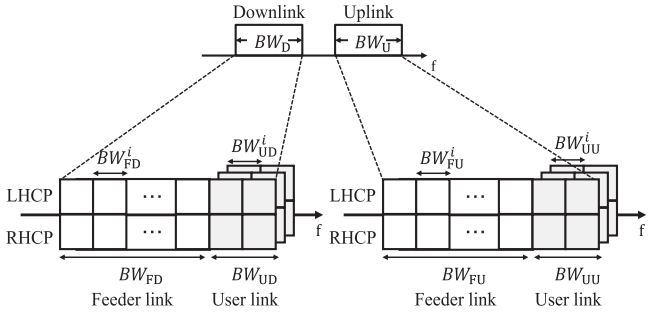

Fig. 5. Frequency allocation.

III. Satellite Communication System Model

In this section, we define the satellite communication system model and note the relationship among factors composing the system. Then, we introduce the channel allocation method for maximizing the traffic accommodation rate.

A. System Model Definition

The frequency bandwidth allocated to downlinking of the satellite communication system is represented as BW_{D}, and the frequency bandwidth for uplinking is represented as BW_{U}. First, we focus on the downlink and summarize the relationship between the frequency bandwidth and channels that are allocated to downlinking. We define the frequency bandwidths for the feeder link and user link as BW_{FD} and BW_{UD}, respectively. Because the summation of the feeder link frequency bandwidth and user link frequency bandwidth is the same as the system frequency bandwidth, these values satisfy the Equation given below:

$$BW_{\mathrm{D}} = BW_{\mathrm{FD}} + BW_{\mathrm{UD}}. \tag{1}$$

The frequency bandwidth of downlinking for GW i is given by BW^i_{FD} and is expressed as follows:

$$\sum_{i=1}^{n_{\mathrm{g}}} BW^i_{\mathrm{FD}} = 2 \cdot BW_{\mathrm{FD}}, \tag{2}$$

where n_{g} is the number of GWs. This model considers polarized waves. Hence, the satellite communication system can use the same frequency bandwidths for right hand circular polarization (RHCP) and left hand circular polarization (LHCP). Therefore, the total frequency bandwidth for the feeder links is double the allocated frequency bandwidth, as illustrated as Fig. 5. In this research, we ignored the effect of polarization loss. The frequency bandwidth of downlinking for beam i is given by

BW^i_{UD} and is expressed as follows:

$$\sum_{i=1}^{n_\mathrm{b}} BW^i_{\mathrm{UD}} = 2 \cdot BW_{\mathrm{UD}} \cdot \left(\frac{n_\mathrm{b}}{n_\mathrm{r}}\right), \tag{3}$$

where n_b is the number of beams and n_r is the number of repetitions of frequency. When the number of repetitions of frequency is n_r, in order to prevent interference between beams, a multi-beam satellite system has to allocate different frequency bandwidths for n_r beams that lie next to each other. However, the multi-beam satellite system can reuse these frequency bandwidths for other beams. When n_r beams that lie next to each other consist of the same group, there are $\frac{n_\mathrm{b}}{n_\mathrm{r}}$ groups in the system. Because a multi-beam satellite can reuse the same frequency bandwidth for these groups, (3) holds true. While the satellite system can use polarized waves in the user link and feeder link, the right side of (3) is doubled. The number of channels for downlinking to GW i is given by CH^i_{FD} and is expressed as follows:

$$CH^i_{\mathrm{FD}} = \frac{BW^i_{\mathrm{FD}}}{bw}, \tag{4}$$

where bw is the frequency bandwidth of the channel. The total number of channels of the feeder link for downlinking is defined as $CH^{\mathrm{all}}_{\mathrm{FD}}$ and is expressed as follows:

$$CH^{\mathrm{all}}_{\mathrm{FD}} = 2 \cdot \frac{BW_{\mathrm{FD}}}{bw}. \tag{5}$$

Then, the following Equation holds true:

$$\sum_{i=1}^{n_\mathrm{g}} CH^i_{\mathrm{FD}} = CH^{\mathrm{all}}_{\mathrm{FD}}. \tag{6}$$

Similar to a feeder link, the number of channels for the user link and the frequency bandwidth that is allocated for the user link have an established relation that is expressed by (7)–(9):

$$CH^i_{\mathrm{UD}} = \frac{BW^i_{\mathrm{UD}}}{bw}, \tag{7}$$

$$CH^{\mathrm{all}}_{\mathrm{UD}} = 2 \cdot \frac{BW_{\mathrm{UD}}}{bw} \cdot \left(\frac{n_\mathrm{b}}{n_\mathrm{r}}\right), \tag{8}$$

$$\sum_{i=1}^{n_\mathrm{b}} CH^i_{\mathrm{UD}} = CH^{\mathrm{all}}_{\mathrm{UD}}, \tag{9}$$

where CH^i_{UD} is the number of channels for downlinking to beam i and $CH^{\mathrm{all}}_{\mathrm{UD}}$ represents all channels that are allocated to the user link for downlinking.

Because the relationship between the frequency bandwidth and channel for uplinking is the same as that for downlinking, the description is omitted.

We define the number of user links that is transmitted by the digital channelizer as n_{uc} and the number of user links that is transmitted by the bent-pipe mode as n_{ub}. Obviously, these two values satisfy (10) given below:

$$n_\mathrm{b} = n_{\mathrm{uc}} + n_{\mathrm{ub}}, \tag{10}$$

In the same manner, we define n_{fc} and n_{fb} for the feeder link. These two values satisfy (11) given below:

$$n_\mathrm{g} = n_{\mathrm{fc}} + n_{\mathrm{fb}}. \tag{11}$$

The number of ports of the digital channelizer is given by n_p and is expressed as follows:

$$n_\mathrm{p} = n_{\mathrm{uc}} + n_{\mathrm{fc}}. \tag{12}$$

The number of channels for traffic from beam i to beam j is defined as ch^{uu}_{ij}, and we summarize all channels that are sent from beam to beam to the matrix as C_{UU}:

$$C_{\mathrm{UU}} = \begin{pmatrix} ch^{\mathrm{uu}}_{1,1} & ch^{\mathrm{uu}}_{1,2} & \cdots & ch^{\mathrm{uu}}_{1,n_\mathrm{b}} \\ ch^{\mathrm{uu}}_{2,1} & ch^{\mathrm{uu}}_{2,2} & \cdots & ch^{\mathrm{uu}}_{2,n_\mathrm{b}} \\ \vdots & \vdots & \ddots & \vdots \\ ch^{\mathrm{uu}}_{n_{\mathrm{uc}},1} & ch^{\mathrm{uu}}_{n_{\mathrm{uc}},2} & \cdots & ch^{\mathrm{uu}}_{n_{\mathrm{uc}},n_\mathrm{b}} \\ ch^{\mathrm{uu}}_{n_{\mathrm{uc}}+1,1} & ch^{\mathrm{uu}}_{n_{\mathrm{uc}}+1,2} & \cdots & ch^{\mathrm{uu}}_{n_{\mathrm{uc}}+1,n_\mathrm{b}} \\ \vdots & \vdots & \ddots & \vdots \\ ch^{\mathrm{uu}}_{n_{\mathrm{uc}}+n_{\mathrm{ub}},1} & ch^{\mathrm{uu}}_{n_{\mathrm{uc}}+n_{\mathrm{ub}},2} & \cdots & ch^{\mathrm{uu}}_{n_{\mathrm{uc}}+n_{\mathrm{ub}},n_\mathrm{b}} \end{pmatrix}. \tag{13}$$

In this matrix, a row represents the source beam, and a column represents the destination beam. When a satellite receives these channels from each beam, the channels are combined in increments of a row for uplinking. The satellite reconstructs these channels in increments of a column for downlinking. Hence, from the first line to the n_{uc}th line are the source beams transmitted by the digital channelizer, and from the $(n_{\mathrm{uc}}+1)$th line to the $(n_{\mathrm{uc}}+n_{\mathrm{ub}})$th line are the source beams transmitted by the bent-pipe mode. Similar to channels that are sent from beam to beam, channels that are sent from the GW to a beam and vice versa are defined as the matrices C_{FU} and C_{UF}, respectively:

$$C_{\mathrm{FU}} = \begin{pmatrix} ch^{\mathrm{fu}}_{1,1} & ch^{\mathrm{fu}}_{1,2} & \cdots & ch^{\mathrm{fu}}_{1,n_\mathrm{b}} \\ ch^{\mathrm{fu}}_{2,1} & ch^{\mathrm{fu}}_{2,2} & \cdots & ch^{\mathrm{fu}}_{2,n_\mathrm{b}} \\ \vdots & \vdots & \ddots & \vdots \\ ch^{\mathrm{fu}}_{n_{\mathrm{fc}},1} & ch^{\mathrm{fu}}_{n_{\mathrm{fc}},2} & \cdots & ch^{\mathrm{fu}}_{n_{\mathrm{fc}},n_\mathrm{b}} \\ ch^{\mathrm{fu}}_{n_{\mathrm{fc}}+1,1} & ch^{\mathrm{fu}}_{n_{\mathrm{fc}}+1,2} & \cdots & ch^{\mathrm{fu}}_{n_{\mathrm{fc}}+1,n_\mathrm{b}} \\ \vdots & \vdots & \ddots & \vdots \\ ch^{\mathrm{fu}}_{n_{\mathrm{fc}}+n_{\mathrm{fb}},1} & ch^{\mathrm{fu}}_{n_{\mathrm{fc}}+n_{\mathrm{fb}},2} & \cdots & ch^{\mathrm{fu}}_{n_{\mathrm{fc}}+n_{\mathrm{fb}},n_\mathrm{b}} \end{pmatrix}, \tag{14}$$

$$C_{\mathrm{UF}} = \begin{pmatrix} ch^{\mathrm{uf}}_{1,1} & ch^{\mathrm{uf}}_{1,2} & \cdots & ch^{\mathrm{uf}}_{1,n_\mathrm{g}} \\ ch^{\mathrm{uf}}_{2,1} & ch^{\mathrm{uf}}_{2,2} & \cdots & ch^{\mathrm{uf}}_{2,n_\mathrm{g}} \\ \vdots & \vdots & \ddots & \vdots \\ ch^{\mathrm{uf}}_{n_{\mathrm{uc}},1} & ch^{\mathrm{uf}}_{n_{\mathrm{uc}},2} & \cdots & ch^{\mathrm{uf}}_{n_{\mathrm{uc}},n_\mathrm{g}} \\ ch^{\mathrm{uf}}_{n_{\mathrm{uc}}+1,1} & ch^{\mathrm{uf}}_{n_{\mathrm{uc}}+1,2} & \cdots & ch^{\mathrm{uf}}_{n_{\mathrm{uc}}+1,n_\mathrm{g}} \\ \vdots & \vdots & \ddots & \vdots \\ ch^{\mathrm{uf}}_{n_{\mathrm{uc}}+n_{\mathrm{ub}},1} & ch^{\mathrm{uf}}_{n_{\mathrm{uc}}+n_{\mathrm{ub}},2} & \cdots & ch^{\mathrm{uf}}_{n_{\mathrm{uc}}+n_{\mathrm{ub}},n_\mathrm{g}} \end{pmatrix}. \tag{15}$$

As a result, all channels are expressed by the following matrix:

$$C = \begin{pmatrix} C_{\mathrm{UU}} & C_{\mathrm{UF}} \\ C_{\mathrm{FU}} & 0 \end{pmatrix}. \tag{16}$$

In the above matrix, 0 represents channels for traffic from the GW to other GWs relayed by the satellite. Because we assumed that each GW is connected to a terrestrial network in this research, traffic from a GW to other GWs by satellite does not exist. Therefore, we set channels for traffic from a GW to other GWs by satellite to 0. When the satellite transmits by bent-pipe mode, it cannot change the number of channels allocated to each destination. If every destination is allocated the same number of channels, the number of channels for each destination is determined as follows:

$$ch_{ij}^{\mathrm{uu}} = \min\left(\left\lfloor \frac{CH_{\mathrm{UU}}^{i}}{n_{\mathrm{b}}+n_{\mathrm{g}}} \right\rfloor, \left\lfloor \frac{CH_{\mathrm{UD}}^{j}}{n_{\mathrm{b}}+n_{\mathrm{g}}} \right\rfloor\right),$$
$$(i = n_{\mathrm{uc}}+1, n_{\mathrm{uc}}+2, \ldots, n_{\mathrm{uc}}+n_{\mathrm{ub}}, j = 1, 2, \ldots, n_{\mathrm{b}}) \tag{17}$$

$$ch_{ij}^{\mathrm{uf}} = \min\left(\left\lfloor \frac{CH_{\mathrm{UU}}^{i}}{n_{\mathrm{b}}+n_{\mathrm{g}}} \right\rfloor, \left\lfloor \frac{CH_{\mathrm{FD}}^{j}}{n_{\mathrm{b}}+n_{\mathrm{g}}} \right\rfloor\right),$$
$$(i = n_{\mathrm{uc}}+1, n_{\mathrm{uc}}+2, \ldots, n_{\mathrm{uc}}+n_{\mathrm{ub}}, j = 1, 2, \ldots, n_{\mathrm{g}}) \tag{18}$$

$$ch_{ij}^{\mathrm{fu}} = \min\left(\left\lfloor \frac{CH_{\mathrm{FU}}^{i}}{n_{\mathrm{b}}+n_{\mathrm{g}}} \right\rfloor, \left\lfloor \frac{CH_{\mathrm{UD}}^{j}}{n_{\mathrm{b}}+n_{\mathrm{g}}} \right\rfloor\right).$$
$$(i = n_{\mathrm{fc}}+1, n_{\mathrm{fc}}+2, \ldots, n_{\mathrm{fc}}+n_{\mathrm{fb}}, j = 1, 2, \ldots, n_{\mathrm{b}}) \tag{19}$$

When the satellite transmits with the digital channelizer, it can change the number of channels allocated to each destination beam and GW. However, although the summation of channels allocated to each destination cannot exceed the number of channels allocated to the source beam or source GW, the channels must meet the following constraints:

$$\sum_{j=1}^{n_{\mathrm{b}}} ch_{ij}^{\mathrm{uu}} + \sum_{j=1}^{n_{\mathrm{g}}} ch_{ij}^{\mathrm{uf}} \le CH_{\mathrm{UU}}^{i},\ (i = 1, 2, \ldots, n_{\mathrm{uc}}) \tag{20}$$

$$\sum_{j=1}^{n_{\mathrm{b}}} ch_{ij}^{\mathrm{fu}} \le CH_{\mathrm{FU}}^{i}.\ (i = 1, 2, \ldots, n_{\mathrm{fc}}) \tag{21}$$

These two constraints are for uplinking. Similar to uplinking, downlinking has the following constraints:

$$\sum_{i=1}^{n_{\mathrm{uc}}} ch_{ij}^{\mathrm{uu}} + \sum_{i=1}^{n_{\mathrm{fc}}} ch_{ij}^{\mathrm{fu}} \le \left\lfloor \frac{CH_{\mathrm{UD}}^{j}}{n_{\mathrm{b}}+n_{\mathrm{g}}} \right\rfloor \cdot n_{\mathrm{p}}, (j = 1, 2, \ldots, n_{\mathrm{b}}) \tag{22}$$

$$\sum_{i=1}^{n_{\mathrm{uc}}} ch_{ij}^{\mathrm{uf}} \le \left\lfloor \frac{CH_{\mathrm{FD}}^{j}}{n_{\mathrm{b}}+n_{\mathrm{g}}} \right\rfloor \cdot n_{\mathrm{p}}.\ (j = 1, 2, \ldots, n_{\mathrm{g}}) \tag{23}$$

In the case of downlinking, the satellite combines channels with the same destination into the same downlink. There are two types of combined channels: those transmitted by the digital channelizer, and those transmitted by the bent-pipe mode. The number of channels transmitted by the bent-pipe mode is previously determined by (17)–(19). Channels transmitted by the digital channelizer can use the remaining number of channels. The right side of (22) and (23) represents the number of channels excluding channels used by the bent-pipe transmission. Table I defines each parameter.

B. Channel Allocation Optimization

As discussed in the previous subsection, we defined the satellite communication system and determined its channel model. In addition, we noted that a digital channelizer can change the number of channels under constraints. We have to consider how to determine the number of channels allocated for each source and destination. In order to determine the number of channels, we used the traffic accommodation rate as an objective function. The traffic accommodation rate T_{acc} is expressed as (24) (25) shown at the bottom of this page.

$$T_{\mathrm{acc}} = \frac{\sum_{i=1}^{n_{\mathrm{b}}}\sum_{j=1}^{n_{\mathrm{b}}} ch_{ij}^{\mathrm{uu}} + \sum_{i=1}^{n_{\mathrm{g}}}\sum_{j=1}^{n_{\mathrm{b}}} ch_{ij}^{\mathrm{fu}} + \sum_{i=1}^{n_{\mathrm{b}}}\sum_{j=1}^{n_{\mathrm{g}}} ch_{ij}^{\mathrm{uf}}}{\sum_{i=1}^{n_{\mathrm{b}}+n_{\mathrm{g}}}\sum_{j=1}^{n_{\mathrm{b}}+n_{\mathrm{g}}} d_{ij}}. \tag{24}$$

$$\text{Flexibility index} = \sum_{\mu=\mu_{\min}}^{\mu_{\max}} \sum_{\Delta\mu=\Delta\mu_{\min}}^{\Delta\mu_{\max}} \left(\frac{1}{\Delta\mu_{\max}-\Delta\mu_{\min}+1}\right) \cdot \left(\frac{1}{\mu_{\max}-\mu_{\min}+1}\right) \cdot (\max T_{\mathrm{acc}}). \tag{26}$$

d_{ij} is the requested number of channels and is defined in (30).

$$D = \begin{pmatrix} d_{1,1} & d_{1,2} & \cdots & d_{1,n_{\mathrm{b}}} & d_{1,n_{\mathrm{b}}+1} & \cdots & d_{1,n_{\mathrm{b}}+n_{\mathrm{g}}} \\ d_{2,1} & d_{2,2} & \cdots & d_{2,n_{\mathrm{b}}} & d_{2,n_{\mathrm{b}}+1} & \cdots & d_{2,n_{\mathrm{b}}+n_{\mathrm{g}}} \\ \vdots & \vdots & \ddots & \vdots & \vdots & \ddots & \vdots \\ d_{n_{\mathrm{b}},1} & d_{n_{\mathrm{b}},2} & \cdots & d_{n_{\mathrm{b}},n_{\mathrm{b}}} & d_{n_{\mathrm{b}},n_{\mathrm{b}}+1} & \cdots & d_{n_{\mathrm{b}},n_{\mathrm{b}}+n_{\mathrm{g}}} \\ d_{n_{\mathrm{b}}+1,1} & d_{n_{\mathrm{b}}+1,2} & \cdots & d_{n_{\mathrm{b}}+1,n_{\mathrm{b}}} & 0 & \cdots & 0 \\ \vdots & \vdots & \ddots & \vdots & \vdots & \ddots & \vdots \\ d_{n_{\mathrm{b}}+n_{\mathrm{g}},1} & d_{n_{\mathrm{b}}+n_{\mathrm{g}},2} & \cdots & d_{n_{\mathrm{b}}+n_{\mathrm{g}},n_{\mathrm{b}}} & 0 & \cdots & 0 \end{pmatrix}. \tag{25}$$

TABLE I
PARAMETER DEFINITION

Number of beams	n_{b}
Number of GWs	n_{g}
Number of repetitions of frequency	n_{r}
Number of user links going through the digital channelizer	n_{uc}
Number of user links going through the bent-pipe part	n_{ub}
Number of feeder links going through the digital channelizer	n_{fc}
Number of feeder links going through the bent-pipe part	n_{fb}
Number of ports of the digital channelizer	n_{p}
Frequency bandwidth of the channel	bw
Frequency bandwidth for uplinking	BW_{U}
Frequency bandwidth for the feeder link (uplinking)	BW_{FU}
Frequency bandwidth for the user link (uplinking)	BW_{UU}
Frequency bandwidth for the feeder link (uplinking) from GW i	BW^{i}_{FU}
Frequency bandwidth for the user link (uplinking) from beam i	BW^{i}_{UU}
Number of channels for the feeder link (uplinking) from GW i	CH^{i}_{FU}
Number of all channels for the feeder link (uplinking)	$CH^{\mathrm{all}}_{\mathrm{FU}}$
Number of channels for the user link (uplinking) from beam i	CH^{i}_{UU}
Number of all channels for the user link (uplinking)	$CH^{\mathrm{all}}_{\mathrm{UU}}$
Frequency bandwidth for downlinking	BW_{D}
Frequency bandwidth for the feeder link (downlinking)	BW_{FD}
Frequency bandwidth for the user link (downlinking)	BW_{UD}
Frequency bandwidth for the feeder link (downlinking) to GW i	BW^{i}_{FD}
Frequency bandwidth for the user link (downlinking) to beam i	BW^{i}_{UD}
Number of channels for the feeder link (downlinking) to GW i	CH^{i}_{FD}
Number of all channels for the feeder link (downlinking)	$CH^{\mathrm{all}}_{\mathrm{FD}}$
Number of channels for the user link (downlinking) to beam i	CH^{i}_{UD}
Number of all channels for the user link (downlinking)	$CH^{\mathrm{all}}_{\mathrm{UD}}$
Number of allocated channels from beam i to beam j	ch^{uu}_{ij}
Number of allocated channels from beam i to GW j	ch^{uf}_{ij}
Number of allocated channels from GW i to beam j	ch^{fu}_{ij}

The traffic accommodation rate represent the rate of channels that the system can allocate to the demand. When this value is close to 1, this means that the system can accommodate a large amount of traffic demand. When a system can allocate the same number of channels against the demand, the traffic accommodation rate is 1. However, the system has to satisfy the constraints shown in (20)–(23), so this value is not always 1.

In this research, a channel allocation method was adopted for the satellite communication system that maximizes the traffic accommodation rate. The number of channels allocated by the system is determined by linear programming [31]. The constraints have already been given in (20)–(23). To maximize the traffic accommodation rate with the requested number of channels given, this is equivalent to maximizing the number of allocated channels while satisfying the constraints, as given in (20)–(23). In addition, to prevent the allocation of more than the number of required channels, we added the following constraints:

$$ch^{\mathrm{uu}}_{ij} \leq d_{ij},\ (i = 1, 2, \ldots, n_{\mathrm{uc}} + n_{\mathrm{ub}}, j = 1, 2, \ldots, n_{\mathrm{b}}) \quad (27)$$

$$ch^{\mathrm{fu}}_{ij} \leq d_{ij},\ (i = 1, 2, \ldots, n_{\mathrm{fc}} + n_{\mathrm{fb}}, j = 1, 2, \ldots, n_{\mathrm{b}}) \quad (28)$$

$$ch^{\mathrm{uf}}_{ij} \leq d_{ij}.\ (i = 1, 2, \ldots, n_{\mathrm{uc}} + n_{\mathrm{ub}}, j = 1, 2, \ldots, n_{\mathrm{g}}) \quad (29)$$

Equations (27)–(29) are conditions for preventing more channels being allocated than requested. Allocation is performed to satisfy the requirement for beam-to-beam, beam-to-GW, and GW-to-beam communications. In the Appendix, we explain about the liner programing.

IV. PERFORMANCE EVALUATION

In this section, we first discuss the flexibility required by a satellite communication system and then explain the system analysis model. Furthermore, we explain the results of our evaluation.

A. Flexibility Analysis Model

The flexibility of a communication system is defined as the system's ability to adapt to changing conditions. Therefore, we have to define these conditions in order to evaluate the flexibility of the system. Evaluations that include condition transition cannot be performed even if it is possible to evaluate the system performance under each condition with the conventional evaluation method. By constructing a system analysis model with parameters that express the state change and system performance, it is possible to evaluate the performance including the condition transition, i.e., flexibility evaluation. In this research, we considered two parameters to determine the conditions. To evaluate the communication system, it is necessary to evaluate the system performance under all possible conditions. This is because highly flexible systems are required to maintain high performance under any condition. Therefore, the evaluation space was determined by setting upper and lower bounds for each parameter. By evaluating the system performance in the evaluation space, we evaluated the flexibility. To compare several systems, we defined an evaluation index that we called the flexibility index. The flexibility index is determined by volume integration of the system performance in the evaluation space. When the flexibility index is close to 1, this means that the system can demonstrate high performance under any condition.

A satellite communication system is required to provide communication for any communication demand. Thus, we adopted the traffic accommodation rate, which is defined in (24), to represent the system performance. To evaluate the improvement in the flexibility, we evaluated the difference in the traffic accommodation rate compared to a bent-pipe system.

B. Parameter Settings

In this analysis, we evaluatedthe extent to which the satellite communication system can accommodate traffic when the traffic to each destination varies. In addition, to investigate the variation in traffic and total traffic, the traffic generated by each beam and GW was defined by using the average value of the number of required channels and the range of variation. We used the average number of required channels μ by the beam and GW and the variance range $\Delta\mu$ in the number of required channels as parameters. Because it directly affects the flexibility of the satellite system, the number of required channels was used as a parameter. For each beam and GW, the number of required channels is generated from $\mu - \Delta\mu$ to $\mu + \Delta\mu$. At this time, the dispersion of traffic is given by the range of variation and the probability of occurrence therein, and the uniform distribution

TABLE II
PARAMETER SETTINGS 1

Number of beams (n_{b})	10
Number of GWs (n_{g})	2
Number of repetitions of the frequency (n_{r})	4
Frequency bandwidth of the channel (bw) [MHz]	2.5
Frequency bandwidth for uplinking (BW_{U}) [MHz]	750
Frequency bandwidth for downlinking (BW_{D}) [MHz]	750
Frequency bandwidth for the feeder link (uplinking) (BW_{FU}) [MHz]	250
Frequency bandwidth for the feeder link (downlinking) (BW_{FD}) [MHz]	250
Frequency bandwidth for the user link (uplinking) (BW_{UU}) [MHz]	500
Frequency bandwidth for the user link (downlinking) (BW_{UD}) [MHz]	500
Frequency bandwidth for the feeder link (uplinking) from GW i (BW^i_{FU}) [MHz]	250
Frequency bandwidth for the user link (uplinking) from beam i (BW^i_{UU}) [MHz]	250
Frequency bandwidth for the feeder link (downlinking) to GW i (BW^i_{FD}) [MHz]	250
Frequency bandwidth for the user link (downlink) to beam i (BW^i_{UD}) [MHz]	250

TABLE III
PARAMETER SETTINGS 2

	Case			
	1	2	3	4
μ	5–15	5–15	8	5
$\Delta\mu$	1	5	1–5	1–5
n_{p}	2,4,6,8,10,12			

gives the largest variation among the set variation range. By setting a distribution with the largest variation for the range of variation, it is possible to evaluate a system that can cope with any state. Thus, we used a uniform distribution. The number of required channels is expressed as follows:

$$\mathbb{D} = \{d_{ij} | \mu - \Delta\mu \leq d_{ij} \leq \mu + \Delta\mu, d_{ij} \in \mathbb{N}\}. \quad (30)$$

The upper bound of the average number of required channels is $\mu_{\max}$, and the lower bound is $\mu_{\min}$. The upper bound of the variance range of the number of required channels is $\Delta\mu_{\max}$, and the lower bound is $\Delta\mu_{\min}$. Then, the flexibility index is expressed by (26). In this analysis, we set $\mu_{\max}$ is 15, $\mu_{\min}$ is 5, $\Delta\mu_{\max}$ is 5, and $\Delta\mu_{\min}$ is 1. Other parameter settings are summarized in Table II. Although it is sufficient for the satellite communication system provider to set appropriate parameters according to the purpose, these values were set as an example for confirming whether the analysis model functions properly.

To evaluate the flexibility index, the total traffic accommodation rate in the evaluation space is needed. Therefore, we evaluated the total traffic accommodation rate in the evaluation space. To clearly show the effect of the average number of required channels and the variance range of the number of required channels on the traffic accommodation rate clearly, we present four different cases with different values of μ and $\Delta\mu$. The combinations of these parameters are summarized in Table III.

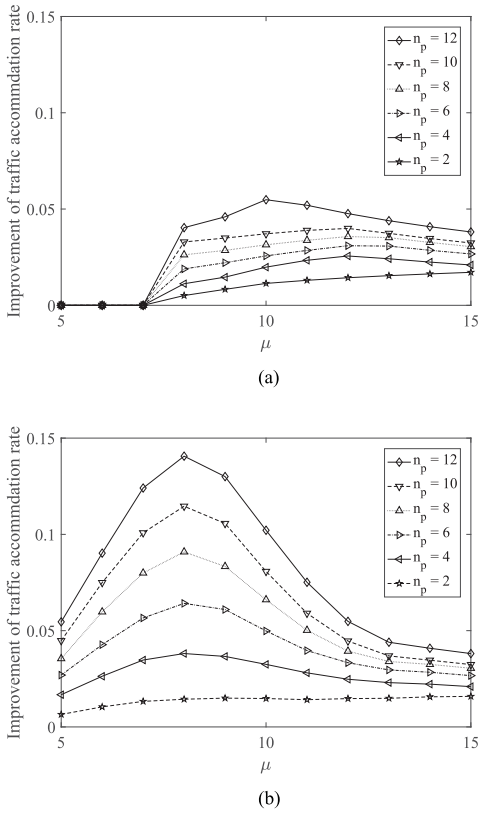

Fig. 6. Improvement in traffic accommodation rate with a fixed $\Delta\mu$. (a) Case 1 ($\Delta\mu = 1$). (b) Case 2 ($\Delta\mu = 5$).

C. Evaluation Results

Figs. 6 and 7 show the differences in the traffic accommodation rate for the bent-pipe satellite system and satellite with a digital channelizer. Fig. 6(a) represents Case 1, where the variance range of the number of required channels is small. This means that the numbers of required channels for the beam and GW are almost the same. In this case, the overall improvement in the traffic accommodation rate is small. In addition, the traffic accommodation rate does not improve at $\mu = 7$. In this analysis, because the frequency bandwidth for the beam and GW is 250 MHz and the frequency bandwidth of a channel is 2.5 MHz, each beam and GW is allocated 100 channels. Each beam and GW allocate these channels to each destination beam and GW, so there are 12 destination beams and GWs. Thus, each destination beam and GW is allocated eight channels by the bent-pipe satellite. Therefore, the bent-pipe satellite can accommodate all traffic unless the number of required channels to each destination beam and GW exceeds 8. In Case 1, when the average number of required channels is 7, the possible number of required channels is 6–8. This is because the variance range of the number of required channels is 1. In this case, the number of required channels does not exceed 8, so the bent-pipe satellite can accommodate all traffic, and the digital channelizer does not improve the traffic accommodation rate. After the average number of required channels becomes 7, the amount of improvement in the traffic accommodation rate increases for all port numbers of the digital channelizer. Then, when the average

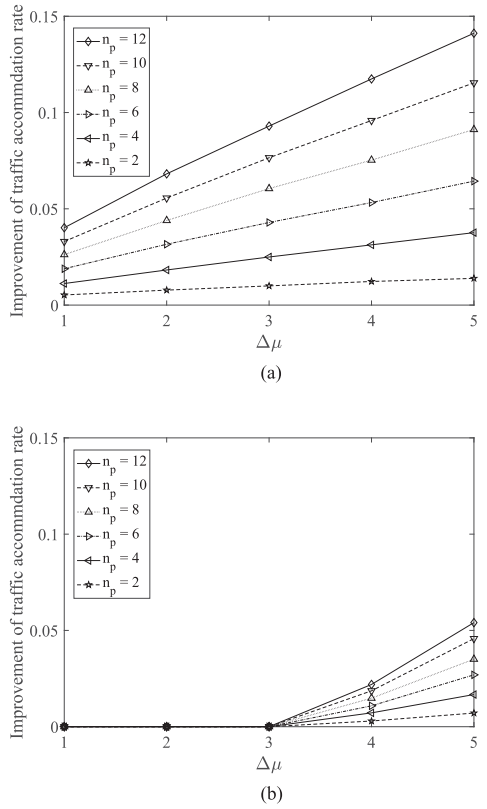

Fig. 7. Improvement in traffic accommodation rate with fixed μ. (a) Case 3 ($\mu = 8$). (b) Case 4 ($\mu = 5$).

number of required channels is further increased, the amount of improvement in the traffic accommodation rate decreases. Because the total number of required channels is large against the improvement in the traffic accommodation rate with the digital channelizer, the improvement in the traffic accommodation rate becomes small. We confirmed that the improvement of the traffic accommodation rate increases with the number of ports of the digital channelizer. Fig. 6(b) represents Case 2, where the variance range of the number of required channels is large. The improvement in the traffic accommodation rate is greater than that of Case 1. This is because the satellite system with the digital channelizer can accommodate greater traffic demand by flexible channel allocation, even if the number of required channels varies widely. Similar to Case 1, as the number of ports of the digital channelizer increases, the traffic accommodation rate improves. The difference in improvement of the traffic accommodation rate with an increasing port number of the digital channelizer is large compared with Case 1. The peak improvement in the traffic accommodation rate is obtained when the average number of required channels is 8. In this case, the total required number of channels is close to the system capacity, and the digital channelizer is used most effectively. Beyond this value, the total required number of channels is too large for both the system with a digital channelizer and the bent-pipe system to accommodate. Thus, the difference in improvement of the traffic accommodation rate decreases.

We now present the results of cases with a fixed average number of required channels and different values for the variance range of the number of required channels. Fig. 7(a) represents

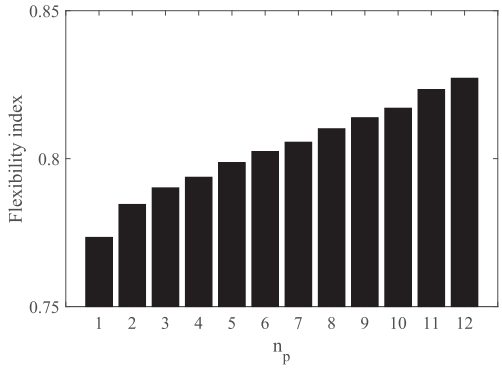

Fig. 8. Flexibility index.

Case 3, where the average number of required channels is 8. This case achieves the highest improvement in traffic accommodation rate as noted previously. The improvement in the traffic accommodation rate increases with the variance range of the number of required channels as well as with the number of ports of the digital channelizer. Fig. 7(b) represents Case 4, where the average number of required channels is 5. In the case of $\mu = 5$, unless the variance in the number of channels exceeds 3, the required channels for each destination beam and GW is not over 8. Thus, the traffic accommodation rate does not improve up to $\Delta\mu = 3$. Even when the variance in the number of channels exceeds 3, the improvement in the traffic accommodation rate is small compared with Case 3. From these results, the improvement in the traffic accommodation rate increases with the variance range of the required number of channels. In addition, when the average required number of channels is large, the improvement in the traffic accommodation rate become large even if the variance range of the required number of channels stays the same. This is because the variance range of the number of required channels has a significant impact when the average number of required channels is close to the system capacity.

Fig. 8 shows the flexibility index, which we presented in a previous subsection. In this research, the number of input antennas (i.e., the sum of the number of beams of the user link and the number of feeder links) was set to 12, so the upper limit of the number of ports of the channelizer was 12. This result shows that the flexibility index increases with the port number of the digital channelizer. In this analysis, because the system with one port for the digital channelizer has the same flexibility index as the bent-pipe system, the results of the bent-pipe satellite have been omitted. When the system has only one port for digital channelizer, the system is strictly limited by the part of the bent-pipe mode, and there is no flexibility. We confirmed that the full channelizer satellite system improves the flexibility index by 5% compared with the bent-pipe system. From the above analysis, we confirmed that the flexibility of a satellite communication system can be quantitatively evaluated with the constructed system analysis model.

V. Conclusion

Although flexibility is strongly required for the next generation of satellite communication systems and the development of technology for flexible utilization of communication resources

is actively ongoing, a system analysis model for quantitatively evaluating flexibility has not been established. In this research, we developed a system analysis model for quantitatively evaluating the flexibility of a satellite communication system and verified the flexibility of a hybrid transponder that shares a digital channelizer and the bent-pipe mode. We showed that the flexibility of hybrid satellite communication system can be quantitatively evaluated with the constructed system analysis model.

APPENDIX

In this section, we describe the algorithm of the linear programming method used to optimize the channel allocation. We consider the following primal linear program:

$$\max \quad \sum_{i=1}^{n} c_i x_i \tag{31}$$

$$\text{s.t.} \quad \sum_{j=1}^{n} a_{ij} x_j \le b_i \ (i = 1, 2, \ldots, m) \tag{32}$$

$$x_i \ge 0 \ (i = 1, 2, \ldots, n) \tag{33}$$

$$b_i \ge 0 \ (i = 1, 2, \ldots, m) \tag{34}$$

Equation (31) represents the objective function, and x_i represents the value to be determined, or the number of allocated channels. (32) represents the constraint condition. In this paper, constraints on the number of uplink channels and constraints on the number of downlink channels correspond to this equation. There are several methods for solving linear programming, but here we explain the simplex method. In the simplex method, the following equations are used to maximize the objective function:

$$N^k(j) = j. \ (j = 1, 2, \ldots, n) \tag{35}$$

$$B^k(i) = n + i. \ (i = 1, 2, \ldots, m) \tag{36}$$

$$D^k = \begin{pmatrix} c_0^k & c_1^k & c_2^k & \ldots & c_n^k \\ b_1^k & a_{11}^k & a_{12}^k & \ldots & a_{1n}^k \\ \vdots & \vdots & \vdots & \ddots & \vdots \\ b_m^k & a_{m1}^k & a_{m2}^k & \ldots & a_{mn}^k \end{pmatrix}. \tag{37}$$

Here, k is a counter representing the number of repetitions. $B^k(i)$ is the suffix of the ith basic variables obtained by the kth iteration, and $N^k(j)$ is the suffix of the jth non-basic variables obtained by the kth iteration. D^k is the coefficient matrix of the dictionary obtained by the kth iteration. First, these values are initialized with k as 0.

A. Step1: Optimality judgment

A suffix s is chosen such that $c_s^k > 0$. If such a suffix does not exist, the maximization of the objective function is achieved, so the algorithm ends here.

B. Step2: Non-solvency judgment

In order to maximize the objective function while satisfying the constraint conditions from the current basic solution, the non-basic variable $x_{N^k(s)}$ is increased as much as possible. That is, a row r satisfying (38) is obtained:

$$-\frac{b_r^k}{a_{rs}^k} = \min\left\{-\frac{b_i^k}{a_{is}^k} : a_{is}^k < 0, 0 \le i \le m\right\}, a_{rs}^k < 0. \tag{38}$$

In the absence of r that satisfies (38), because the objective function is increased without an upper bound, the line programming method ca not be solved, so the algorithm is terminated. When r exists, a pivot operation centered on (r, s) is performed. D^k before the pivot operation is performed as expressed by (39), and D^{k+1} after the pivot operation is expressed by (40) shown at the bottom of this page.

$$D^k = \begin{pmatrix} c_0^k & \ldots & c_s^k & \ldots & c_j^k & \ldots & c_n^k \\ \vdots & & \vdots & & \vdots & & \vdots \\ b_r^k & \ldots & a_{rs}^k & \ldots & a_{rj}^k & \ldots & a_{rn}^k \\ \vdots & & \vdots & & \vdots & & \vdots \\ b_i^k & \ldots & a_{is}^k & \ldots & a_{ij}^k & \ldots & a_{in}^k \\ \vdots & & \vdots & & \vdots & & \vdots \\ b_m^k & \ldots & a_{ms}^k & \ldots & a_{mj}^k & \ldots & a_{mn}^k \end{pmatrix}. \tag{39}$$

Then, N^{k+1} and B^{k+1} are set as follows, and the procedure returns to step 1 with k as $k + 1$.

$$N^{k+1}(s) = B^k(r). \tag{41}$$

$$B^{k+1}(r) = N^k(s). \tag{42}$$

$$D^{k+1} = \begin{pmatrix} c_0^k - \frac{b_r^k}{a_{rs}^k} c_s^k & \ldots & \frac{c_s^k}{a_{rs}^k} & \ldots & c_j^k - \frac{b_r^k}{a_{rs}^k} c_s^k & \ldots & c_n^k - \frac{b_r^k}{a_{rs}^k} c_s^k \\ \vdots & & \vdots & & \vdots & & \vdots \\ -\frac{b_r^k}{a_{rs}^k} & \ldots & -\frac{1}{a_{rs}^k} & \ldots & -\frac{a_{rj}^k}{a_{rs}^k} & \ldots & -\frac{a_{rn}^k}{a_{rs}^k} \\ \vdots & & \vdots & & \vdots & & \vdots \\ b_i^k - \frac{a_{is}^k}{a_{rs}^k} b_r^k & \ldots & \frac{a_{is}^k}{a_{rs}^k} & \ldots & a_{ij}^k - \frac{a_{is}^k}{a_{rs}^k} a_{rj}^k & \ldots & a_{in}^k - \frac{a_{is}^k}{a_{rs}^k} a_{rn}^k \\ \vdots & & \vdots & & \vdots & & \vdots \\ b_m^k - \frac{a_{ms}^k}{a_{rs}^k} b_r^k & \ldots & \frac{a_{ms}^k}{a_{rs}^k} & \ldots & a_{mj}^k - \frac{a_{ms}^k}{a_{rs}^k} a_{rj}^k & \ldots & a_{mn}^k - \frac{a_{ms}^k}{a_{rs}^k} a_{rn}^k \end{pmatrix}. \tag{40}$$

$$N^{k+1}(j) = N^k(j). \ (\forall j \neq s) \tag{43}$$

$$B^{k+1}(i) = B^k(i). \ (\forall i \neq r) \tag{44}$$

By advancing the calculation like this, x_i that maximizes the objective function can be obtained.

REFERENCES

[1] C. Perera, C. H. Liu, S. Jayawardena, and M. Chen, "A survey on Internet of Things from industrial market perspective," *IEEE Access*, vol. 2, pp. 1660–1679, 2014.

[2] J. A. Stankovic, "Research directions for the Internet of Things," *IEEE Internet Things J.*, vol. 1, no. 1, pp. 3–9, Feb. 2014.

[3] Y. Kawamoto, Z. Md. Fadlullah, H. Nishiyama, N. Kato, and M. Toyoshima, "Prospects and challenges of context-aware multimedia content delivery in cooperative satellite and terrestrial networks," *IEEE Commun. Mag.*, vol. 52, no. 6, pp. 55–61, Jun. 2014.

[4] Y. Kawamoto, H. Nishiyama, Z. Md. Fadlullah, and N. Kato, "Effective data collection via satellite-routed sensor system (SRSS) to realize global-scaled Internet of Things," *IEEE Sensors J.*, vol. 13, no. 10, pp. 3645–3654, Oct. 2013.

[5] W. Kong *et al.*, "A ground-based optical system for autonomous landing of a fixed wing UAV," in *Proc. 2014 IEEE/RSJ Int. Conf. Intell. Robots Syst.*, Nov. 2014, pp. 4797–4804.

[6] W. Harbison and R. Gupta, "Long range inter-band radio with the processed surrogate satellite waveform," in *Proc. IEEE Mil. Commun. Conf.*, Oct. 2014, pp. 507–512.

[7] C. McLain, S. Panthi, M. Sturza, and J. Hetrick, "High throughput Ku-band satellites for aeronautical applications," in *Proc. IEEE Mil. Commun. Conf.*, 2012, pp. 1–6.

[8] Y. Kawamoto, H. Nishiyama, N. Kato, and N. Kadowaki, "A traffic distribution technique to minimize packet delivery delay in multi-layered satellite networks," *IEEE Trans. Veh. Technol.*, vol. 62, no. 7, pp. 3315–3324, Sep. 2013.

[9] H. Nishiyama, Y. Tada, N. Kato, N. Yoshimura, M. Toyoshima, and N. Kadowaki, "Toward optimized traffic distribution for efficient network capacity utilization in two-layered satellite networks," *IEEE Trans. Veh. Technol.*, vol. 62, no. 3, pp. 1303–1313, Mar. 2013.

[10] K. Kaneko, Y. Kawamoto, H. Nishiyama, N. Kato, and M. Toyoshima, "An efficient utilization of intermittent surface-satellite optical links by using mass storage device embedded in satellites," *Perform. Eval.*, vol. 87, pp. 37–46, May 2015.

[11] H. Fenech, S. Amos, A. Tomatis, and V. Soumpholphakdy, "High throughput satellite systems: An analytical approach," in *Proc. IEEE Trans. Aeros. Electron. Syst.*, vol. 51, no. 1, pp. 192–202, Jan. 2015.

[12] L. Del Consuelo Hernandez Ruiz Gaytan, Z. Pan, J. Liu, and S. Shimamoto, "Dynamic scheduling for high throughput satellites employing priority code scheme," *IEEE Access*, vol. 3, pp. 2044–2054, Oct. 2015.

[13] D. Giggenbach, E. Lutz, J. Poliak, R. Mata-Calvo, and C. Fuchs, "A high-throughput satellite system for serving whole europe with fast internet service, employing optical feeder links," in *Proc. 9th ITG Symp. Broadband Coverage Germany*, Apr. 2015, pp. 1–7.

[14] A. Botta and A. Pescape, "On the performance of new generation satellite broadband internet services," in *IEEE Commun. Mag.*, vol. 52, no. 6, pp. 202–209, Jun. 2014.

[15] C. McLain, S. Panthi, M. Sturza, and J. Hetrick, "High throughput Ku-band satellites for aeronautical applications," in *Proc. IEEE Mil. Commun. Conf.*, Oct./Nov. 2012, pp. 1–6.

[16] S. Dimitrov, S. Erl, B. Barth, S. Jaeckel, A. Kyrgiazos, and B. G. Evans, "Radio resource management techniques for high throughput satellite communication systems," in *Proc. Eur. Conf. Netw. Commun.*, Jun./Jul. 2015, pp. 175–179.

[17] D. Serrano-Velarde, E. Lance, H. Fenech, and G. E. Rodriguez-guisantes, "Novel dimensioning method for high-throughput satellites: Forward link," *IEEE Trans. Aerosp. Electron. Syst.*, vol. 50, no. 3, pp. 2146–2163, Jul. 2014.

[18] S. Tani, K. Motoyoshi, H. Sano, A. Okamura, H. Nishiyama, and N. Kato, "Flexibility-enhanced HTS system for disaster management: Responding to communication demand explosion in a disaster," *IEEE Trans. Emerg. Topics Comput.*, doi: 10.1109/TETC.2017.2688078, to be published.

[19] J. Cherkaoui and V. Glavac, "Signal frequency channelizer/synthesizer," in *Proc. 10th Int. Workshop Signal Process. Space Commun.*, Oct. 2008, pp. 1–4.

[20] Y. Fujino, T. Orikasa, and N. Hamamoto, "Measurement experiment of deployable large scale reflector antenna with DBF using A-METLAB," in *Proc. IEEE MTT-S Int. Microw. Workshop Series Innov. Wireless Power Transm. Technol. Syst. Appl.*, May 2012, pp. 159–162.

[21] H. Yang, J.-H. Dang, Y.-H. Pan, and Z.-K. Li, "A digital channelizer design approach for broadband satellite communications based on frequency domain filter theory," in *Proc. Int. Conf. Mechatronic Sci., Electric Eng. Comput.*, Dec. 2013, pp. 2986–2990.

[22] Y. Fujino, H. Tsuji, N. Komiyama, and T. Orikasa, "Experimental study for DBF and channelizer for satellite/terrestrial integrated mobile communication system," in *Proc. Int. Symp. Antennas Propag.*, Nov. 2012, pp. 720–723.

[23] J. Lei and M. Vzquez-Castro, "Multibeam satellite frequency/time duality study and capacity optimization," *J. Commun. Netw.*, vol. 13, no. 5, pp. 472–480, Oct. 2011.

[24] C. Morel, P. D. Arapoglou, M. Angelone, and A. Ginesi, "Link adaptation strategies for next generation satellite video broadcasting: A system approach," *IEEE Trans. Broadcast.*, vol. 61, no. 4, pp. 603–614, Dec. 2015.

[25] X. Kan and X. Xu, "Energy- and spectral-efficient power allocation in multi-beam satellites system with co-channel interference," in *Proc. Int. Conf. Wireless Commun. Signal Process.*, Oct. 2015, pp. 1–6.

[26] Y. Ding, Y. C. Jiao, L. Zhang, and B. Li, "Solving port selection problem in multiple beam antenna satellite communication system by using differential evolution algorithm," *IEEE Trans. Antennas Propag.*, vol. 62, no. 10, pp. 5357–5361, Oct. 2014.

[27] W. Wang, R. Wang, Y. Deng, W. Xu, and L. Hou, "Improved digital beam-forming approach with scaling function for range multi-channel synthetic aperture radar system," *IET Radar, Sonar Navig.*, vol. 10, no. 2, pp. 379–385, Feb. 2016.

[28] S. Tani, K. Motoyoshi, H. Sano, A. Okamura, H. Nishiyama, and N. Kato, "An adaptive beam control technique for Q band satellite to maximize diversity gain and mitigate interference to terrestrial networks," *IEEE Trans. Emerging Top. Comput.*, doi: 10.1109/TETC.2016.2606107, to be published.

[29] P. Takats and P. Garland, "Evolution of regional multimedia satellite architectures," in *Proc. IEEE Aerosp. Conf.*, Mar. 2000, vol. 1, pp. 255–260.

[30] A. Markhasin, "Satellite-based fully distributed mesh hybrid networking technology DVB-S2/RCS-WiMAX for RRD areas," in *Proc. 5th Adv. Satell. Multimedia Syst. Conf. 11th Signal Process. Space Commun. Workshop*, Sep. 2010, pp. 294–300.

[31] I. Koutsopoulos and P. Constantinou, "Joint channel estimation and satellite antenna power control in mobile satellite networks using ray tracing," in *Proc. IEEE 51st Veh. Technol. Conf. Proc.*, May 2000, vol. 2, pp. 1586–1590.

Kazuma Kaneko (GS'12) received the B.E. degree from the Information Engineering in 2013, and M.S. degree in 2015 from the Graduate School of Information Science (GSIS), Tohoku University, Sendai, Japan, where he is currently working toward the Ph.D. degree in the GSIS. He received the Best Paper Award at the IEEE International Conference on Communications in 2017. He also received the 2014 IEEE ComSoc Sendai Chapter Student Excellent Research Award, the prestigious Deans Awards from Tohoku University in 2015, Japan Society for the Promotion of Science Fellowship in 2016.

Hiroki Nishiyama (SM'13) received the M.S. and Ph.D. degree in information science from Tohoku University, Sendai, Japan, in 2007 and 2008, respectively. He is an Associate Professor in the Graduate School of Information Sciences, Tohoku University. He has published more than 170 peer-reviewed papers including many high quality publications in prestigious IEEE journals and conferences. His research interests include a wide range of areas including satellite communications, unmanned aircraft system networks, wireless and mobile networks, ad hoc and sensor networks, green networking, and network security. One of his outstanding achievements is Relay-by-Smartphone, which makes it possible to share information among many people by device-to-device direct communication. He received Best Paper Awards from many international conferences including IEEE's flagship events, such as the IEEE Global Communications Conference in 2014 (GLOBECOM'14), GLOBECOM'13, GLOBECOM'10, the IEEE International Conference on Communications in 2016, and the IEEE Wireless Communications and Networking Conference in 2012 (WCNC'12), WCNC'14. He also received the 2017 FUNAI Foundation's Academic Award for Information Technology, the Special Award of the 29th Advanced Technology Award for Creativity in 2015, the IEEE Communications Society Asia-Pacific Board Outstanding Young Researcher Award 2013, and the IEICE Communications Society Academic Encouragement Award 2011. He is currently an Associate Editor for Springer Journal of Peer-to-Peer Networking and Applications, and the Secretary of IEEE ComSoc Sendai Chapter. He is a senior member of Institute of Electronics, Information and Communication Engineers.

Nei Kato (F'13) received the Bachelor's degree from Polytechnic University—Japan, Sagamihara, Japan, in 1986, and the M.S. and Ph.D. degrees in information engineering from Tohoku University, Sendai, Japan, in 1988 and 1991, respectively. He joined the Computer Center of Tohoku University as an Assistant Professor in 1991, and was promoted to a Full Professor in Graduate School of Information Sciences, Tohoku University, in 2003. He became a Strategic Adviser to the President of Tohoku University in 2013 and the Director of Research Organization of Electrical Communication, Tohoku University, in 2015. He has published more than 300 papers in peer-reviewed journals and conference proceedings. His research interests include computer networking, wireless mobile communications, satellite communications, ad hoc and sensor and mesh networks, smart grid, and pattern recognition. He currently serves as a Member-at-Large on the Board of Governors, the IEEE Communications Society, the Chair of IEEE ComSoc Sendai Chapter, a Vice Chair of Fellow Committee of IEEE Computer Society (2016), member of IEEE ComSoc Award Committee (2015–2017), the Editor-in-Chief of the IEEE Network Magazine since 2015, the Associate Editor-in-Chief of IEEE INTERNET OF THINGS JOURNAL, an Area Editor of the IEEE TRANSACTIONS ON VEHICULAR TECHNOLOGY. He was the Chair of Satellite and Space Communications Technical Committee (2010–2012) and Ad Hoc and Sensor Networks Technical Committee (2014–2015) of the IEEE ComSoc, respectively, the Chair of IEICE Satellite Communications Technical Committee (2011–2012). He received Minoru Ishida Foundation Research Encouragement Prize (2003), Distinguished Contributions to Satellite Communications Award from the IEEE Communications Society, Satellite and Space Communications Technical Committee (2005), the FUNAI information Science Award (2007), the TELCOM System Technology Award from Foundation for Electrical Communications Diffusion(2008), the IEICE Network System Research Award (2009), the IEICE Satellite Communications Research Award (2011), the KDDI Foundation Excellent Research Award (2012), IEICE Communications Society Distinguished Service Award (2012), Distinguished Contributions to Disaster-resilient Networks R&D Award from Ministry of Internal Affairs and Communications, Japan (2014), seven Best Paper Awards from IEEE GLOBECOM/WCNC/VTC, and IEICE Communications Society Best Paper Award (2012). Besides his academic activities, he also serves on the Expert Committee of Telecommunications Council, Ministry of Internal Affairs and Communications, and as the Chairperson of ITU-R SG4 and SG7, Japan. He is currently a Distinguished Lecturer of the IEEE Communications Society and Vehicular Technology Society. He is a Fellow the Institute of Electronics, Information and Communication Engineers.

Amane Miura (M'00) received the Ph.D. degree in information sciences from Tohoku University, Sendai, Japan, in 1998. Since 1998, he has been with the Communications Research Laboratory, Tokyo, Japan, now reorganized as the National Institute of Information and Communications Technology (NICT), to engage in the research on satellite communications and antennas. He is currently a Senior Researcher in the NICT. He is a member of Institute of Electronics, Information and Communication Engineers, and a Committee Member of Space Communications and Navigation for IAF.

Morio Toyoshima (M'02) received the B.S. and M.S. degrees in electronic engineering from Shizuoka University, Shizuoka, Japan, in 1992 and 1994, respectively. He received the Ph.D. degree in electronic engineering from the University of Tokyo, Tokyo, Japan, in 2003. He joined the Communications Research Laboratory (CRL, Ministry of Posts and Telecommunications) in 1994 and soon after was engaged in research for the Engineering Test Satellite VI (ETS-VI) optical communication experiment. He was later involved in the Ground-to-Orbit Lasercomm Demonstration (GOLD) experiment with NASA's Jet Propulsion Laboratory. He joined the Japan Aerospace Exploration Agency (formerly, NASDA) to assist in the development of the Optical Inter-Orbit Communications Engineering Test Satellite (OICETS), from 1999 to 2003. In December 2003, he became a Senior Researcher in the Optical Space Communications Group (NICT; formerly CRL), Japan. Starting in October 2004, he spent one year as a Guest Scientist at Vienna University of Technology, Austria, in the field of optical space communications. In April 2006, he returned to NICT, where he conducted ground-to-OICETS laser communication experiments in 2006. He was involved in the development of the Small Optical TrAnsponder for 50-kg-class satellites. He was a Visiting Professor in the Graduate School of Information Systems, the University of Electro-Communications, from 2007 to 2013. He was the Director of the Space Communication Systems Laboratory, the Wireless Network Research Institute in NICT, from 2011 to 2016. He is currently the Director of the Space Communications Laboratory, the Wireless Networks Research Center in NICT, since April 2016. His research interests include laser beam propagation through atmospheric turbulence, space laser communications, and quantum cryptography. He received the Minister of Posts and Telecommunications Award on April 20, 1996, as part of the ETS-VI Satellite Experiment Group and an Annual NASA Honor Award on May 28, 1997 as part of the GOLD Team.